

## An engineered HIV-1 gp41 trimeric coiled coil with increased stability and anti-HIV-1 activity: implication for developing anti-HIV microbicides

Pei Tong<sup>1†</sup>, Zhifeng Lu<sup>1†</sup>, Xi Chen<sup>1</sup>, Qian Wang<sup>2</sup>, Fei Yu<sup>3</sup>, Peng Zou<sup>3</sup>, Xiaoxia Yu<sup>4</sup>, Yu Li<sup>1</sup>, Lu Lu<sup>2,3‡</sup>, Ying-Hua Chen<sup>1‡</sup> and Shibo Jiang<sup>2,3\*‡</sup>

<sup>1</sup>School of Life Sciences, Tsinghua University, Key Laboratory for Protein Sciences of MOE, Beijing 100084, China; <sup>2</sup>Key Laboratory of Medical Molecular Virology of Ministries of Education and Health, Shanghai Medical College and Institute of Medical Microbiology, Fudan University, Shanghai 200032, China; <sup>3</sup>Lindsley F. Kimball Research Institute, New York Blood Center, New York, NY 10065, USA; <sup>4</sup>Institute of Biophysics, Chinese Academy of Sciences, Beijing 100101, China

\*Corresponding author. Tel: +86-021-54237673; Fax: +86-021-54237465; E-mail: shibojiang@fudan.edu.cn

†These authors contributed equally.

‡These authors contributed equally.

Received 28 January 2013; returned 30 April 2013; revised 3 May 2013; accepted 15 May 2013

**Objectives:** We previously constructed a trimeric coiled coil, N28Fd, based on the N-heptad repeat (NHR) sequence of HIV-1 gp41, as a promising HIV-1 entry inhibitor. Here, we attempted to engineer a stabilized trimeric coiled coil, ccN28Fd, by adding interchain disulphide bonds at the N terminus of N28Fd to improve its biophysical properties and anti-HIV-1 efficacy.

**Methods:** Molecular biology techniques were applied to engineer ccN28Fd. Circular dichroism and sedimentation velocity analysis were used to determine its secondary structure and thermostability and polymeric states, respectively. The anti-HIV-1 activity was assessed by p24 or luciferase expression. Its cytotoxicity was evaluated by XTT assay.

**Results:** At low pH, ccN28Fd and N28Fd were in trimeric and monomeric conformation, respectively. ccN28Fd showed higher thermostability and much stronger antiviral activity against HIV-1 IIIB (X4) and Bal (R5) strains than N28Fd. ccN28Fd was effective in inhibiting infection by a broad spectrum of primary HIV-1 isolates and enfuvirtide-resistant strains and blocking cell-to-cell HIV-1 transmission. A combination of ccN28Fd with tenofovir, a nucleoside reverse transcriptase inhibitor-based microbicide, exhibited potent synergistic anti-HIV-1 activity. ccN28Fd was highly resistant to digestion by proteinase K at pH 7.2 and pepsin at pH 1.5, and its anti-HIV-1 activity was not significantly affected by the presence of hydroxyethyl cellulose gel, seminal fluid or vaginal fluid simulant. It possessed no significant *in vitro* cytotoxicity.

**Conclusions:** The engineered ccN28Fd maintains high stability in a low pH environment and exhibits potent and broad anti-HIV-1 activity, suggesting good potential for development as an effective and safe vaginal microbicide to prevent HIV sexual transmission.

**Keywords:** N-heptad repeat, trimer, disulphide bonds, enfuvirtide, tenofovir

### Introduction

Unprotected heterosexual contact is the primary mode of HIV transmission in developing countries, and it is becoming an increasing risk factor in developed countries.<sup>1</sup> Most new infections among women in Asia are contracted from their husbands.<sup>2</sup> Hence, it is of great importance to develop microbicides to prevent sexual transmission of HIV.

Previous studies focused on the development of the non-specific anionic polymer-based microbicides, such as naphthalene sulfonate (PRO2000),<sup>3,4</sup> carrageenan (Carraguard)<sup>5,6</sup> and cellulose sulphate (Ushercell).<sup>7–9</sup> These microbicides inhibit HIV entry into host cells by interacting with the HIV envelope proteins (Env), mainly through anionic interaction and the disruption of HIV attachment to CD4<sup>+</sup> cells. Unfortunately, results from clinical trials showed that they failed to demonstrate efficacy in preventing

HIV-1 acquisition, partially because of their limited efficacy against CCR5-tropic HIV-1 strains, which constitute the most common phenotype transmitted by the sexual route.<sup>10,11</sup>

Recent studies have shifted towards developing microbicides based on the small-molecule HIV reverse transcriptase inhibitors (RTIs), including nucleoside reverse transcriptase inhibitors (NRTIs), such as tenofovir,<sup>12,13</sup> and non-nucleoside reverse transcriptase inhibitors (NNRTIs), e.g. TMC-120.<sup>14,15</sup> A Phase IIb clinical trial (CAPRISA 004 trial) of 1% tenofovir clinical trial gel as a microbicide in South Africa showed that participants who used tenofovir gel before and after sex exhibited lower HIV acquisition with, an estimated reduction of 39% overall and 54% with high gel adherence.<sup>16</sup> However, RTI-based microbicides may not be effective against RTI-resistant HIV-1 strains. RTIs, as the major components in antiretroviral therapy (ART), have been widely used in clinics. Therefore, many HIV-1 isolates are already resistant to RTIs when they are transmitted from ART-treated HIV-1-infected patients to uninfected persons. Therefore, development of microbicide combinations consisting of RTIs and HIV-1 entry inhibitors is urgently needed for preventing HIV sexual transmission.<sup>17</sup>

The first HIV-1 entry inhibitor approved by the US FDA for treating HIV-1-infected patients who failed to respond to the current ART was enfuvirtide (brand name Fuzeon, generic name enfuvirtide), which is a synthetic peptide derived from the C-terminal heptad repeat (CHR) region of HIV-1 gp41.<sup>18–20</sup> Enfuvirtide and other CHR peptides, such as C52-L,<sup>21</sup> sifuvirtide<sup>22</sup> and L644,<sup>23</sup> have been used for developing anti-HIV microbicides. However, CHR peptides are unstructured in solution according to biophysical and structure analysis, and they are unstable in the vaginal environment, which has a low pH (3.8–4.4) and abundant proteolytic

enzymes.<sup>24–27</sup> Therefore, it is preferable to develop microbicides based on a trimeric coiled coil formed by the peptides derived from the N-terminal heptad repeat (NHR) region. The NHR trimers inhibit HIV fusion by binding to the viral gp41 CHRs<sup>28–30</sup> or by disrupting the formation of inner NHR trimers.<sup>31</sup>

We previously designed an NHR trimer, designated N28Fd, consisting of a 28-mer NHR peptide fused with a T4 fibrin trimerization motif, foldon (Fd), as an anti-HIV-1 microbicide. Compared with the original N28 peptide, N28Fd showed much improved anti-HIV-1 potency.<sup>25</sup> However, we found N28Fd to be sensitive to proteolytic enzymes and low pH and that it had lower anti-HIV-1 activity than enfuvirtide. Therefore, in this study, we introduced intermolecular disulphide bonds by adding two cysteines at the N terminus of N28Fd in order to stabilize the trimeric coiled coil (Figure 1). As expected, this newly engineered recombinant protein, designated ccN28Fd, exhibited much improved thermostability and resistance to proteolytic enzymes and low pH. Its anti-HIV-1 activity was significantly improved ~10-fold over that of N28Fd. Seminal fluid (SF) and vaginal fluid simulant (VFS) had no effect on its antiviral potency. Combining ccN28Fd with tenofovir resulted in strong synergism. These results suggest that ccN28Fd can be further developed as an effective and stable component in a novel microbicide combination.

## Materials and methods

### Reagents

Peptides C34 (amino acids 628–661) and enfuvirtide (amino acids 638–673) were synthesized by a standard solid-phase Fmoc [N-(9-fluorenyl)]

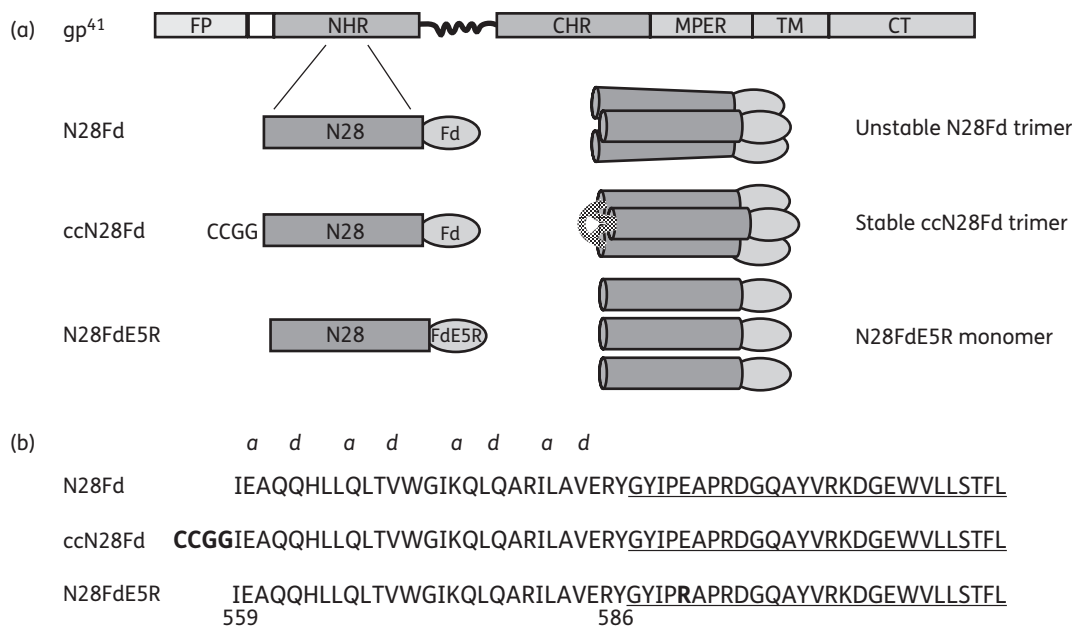


**Figure 1.** Design of ccN28Fd based on the HIV-1 gp41 NHR sequence. (a) Schematic presentation of gp41, N28Fd and its derivatives. The gp41 consists of fusion peptide (FP), NHR, loop region, CHR, membrane-proximal external region (MPER), transmembrane domain (TM) and cytoplasm tail (CT). ccN28Fd may form a more stable trimeric coiled coil than N28Fd because of the presence of three intermolecular disulphide bonds at its N terminus, while N28FdE5R may become monomeric because of the E5R mutation in Fd. (b) The amino acid sequences of N28Fd, ccN28Fd and N28FdE5R. The residue number corresponds to its position in HIV-1 HXB2 gp160. The sequences of Fd are underlined. The letters 'a' and 'd' indicate the positions of the corresponding residues in the helical wheel of the gp41 NHR domain. The added residues of ccN28Fd and the mutation of E5R are highlighted in bold.

methoxycarbonyl method as described previously.<sup>32</sup> Both peptides bear an acetyl group at the N terminus and an amide group at the C terminus. The peptides were purified to homogeneity (>95% purity) by HPLC and verified by mass spectrometry. Proteinase K-agarose, pepsin, phytohaemagglutinin (PHA), interleukin-2 (IL-2) and XTT were purchased from Sigma (St Louis, MO, USA). SF was purchased from Lee Biosolutions, Inc. (St Louis, MO, USA). VFS was prepared as described by Owen and Katz.<sup>33</sup> GFP (green fluorescent protein)-transduced human osteosarcoma (Ghost) cells, which express CD4 and coreceptors CCR5 and CXCR4, were kindly provided by Dr Linqi Zhang at Tsinghua University. The cells (HEK 293T, MT-2 and TZM-bl), the anti-HIV drug tenofovir, the laboratory-adapted HIV-1 strains IIIB and Bal, and the primary HIV-1 isolates, as well as the HIV-1 enfuvirtide-resistant strains, including NL4-3(36G)V38A, NL4-3(36G)V38A/N42D, NL4-3(36G)N42T/N43K, NL4-3(36G)V38A/N42T and NL4-3(36G)V38E/N42S, and the plasmids (pNL4-3.Luc.R'E' and pHXB2-Env) were obtained from the NIH AIDS Research and Reference Reagent Program. VK2/E6E7 cells were purchased from ATCC (Manassas, VA, USA).

### Plasmid construction

The plasmid encoding N28Fd was constructed as described previously<sup>25</sup> and used to create the vectors encoding ccN28Fd and N28FdE5R, respectively, using a standard point mutation method by PCR. The resultant ccN28Fd should contain four residues (CCGG) at the N terminus of N28Fd, while N28FdE5R should bear a Glu (E) → Arg (R) mutation at the fifth residue of Fd. The DNA fragments were cloned into the BamHI and XhoI sites of pGEX-6p-1 vector (GE Healthcare, Sweden).

### Expression and purification of the recombinant proteins

Each of the recombinant plasmids was transformed into *Escherichia coli* strain Rosetta. The recombinant protein N28Fd was induced at 30°C with 0.4 mM IPTG for 5 h, while ccN28Fd and N28FdE5R were induced at 16°C for 12 h. The recombinant proteins with glutathione S-transferase (GST) tags were first purified with a standard procedure using glutathione Sepharose 4B Fast flow beads (GE Healthcare, Sweden), followed by further purification on a Superdex-200 column (GE Healthcare, Sweden) with elution buffer of acetic acid-sodium acetate solution (100 mM, pH 5.0). For ccN28Fd, oxidation was performed by adding oxidized and reduced glutathione to final concentration of 9 mM and 0.9 mM, respectively. After 5 days, the protein was dialysed against appropriate buffer. The purified proteins were analysed with SDS-PAGE, and their concentrations were determined with absorbance at UV280.

### Sedimentation velocity analysis (SVA)

All measurements were performed on the Proteomelab™XL-A/XL-I analytical ultracentrifuge (Beckman Coulter, Fullerton, CA, USA) at 20°C as previously described.<sup>25</sup> In brief, three-channel cells were used with an An-60 Ti rotor. The recombinant proteins were dialysed against acetic acid/sodium acetate solution (100 mM, pH 6.0). Each of the proteins was mixed with equimolar C34 in PBS (150 mM Na<sub>2</sub>HPO<sub>4</sub>, 2.5 mM NaH<sub>2</sub>PO<sub>4</sub>, and 150 mM NaCl, pH 7.2) and incubated at 37°C for 30 min. All samples were prepared at final concentration of 50 μM and were initially scanned at 3000 rpm for 10 min to identify the appropriate wavelength for data collection. Data were collected at 60 000 rpm at wavelengths of 280 nm. Sedimentation coefficient distribution, *c* (s), and molecular mass distribution, *c* (M), were calculated using the SEDFIT program.

### Circular dichroism (CD) analysis

The secondary structure and a melting temperature (*T<sub>m</sub>*) of the recombinant proteins were analysed by CD spectroscopy as previously described.<sup>34</sup> Briefly, the individual proteins and their mixtures with C34 peptide (at

equimolar concentration) were prepared in PBS at final concentration of 10 μM and incubated at 37°C for 30 min. Data were acquired on an Applied Photophysics Pi-Star 180 spectropolarimeter (Applied Photophysics, UK) at a 3 nm bandwidth, 0.1 nm resolution, 0.1 cm path length, 1 nm wavelength interval from 200 to 260 nm and corrected by subtraction of a blank corresponding to the solvent. The content of α-helix was determined from the CD signal by dividing the mean residue ellipticity at 222 nm by the value expected for 100% helix formation (33 000 degrees cm<sup>2</sup> dmol<sup>-1</sup>).<sup>35</sup> Thermal denaturation of the recombinant proteins and their complexes with C34 peptide was assessed at 208 nm by monitoring a temperature gradient from 15°C to 90°C with a 1°C interval.

### Analysis of single-cycle pseudovirus infection

Single-cycle pseudovirus infection assay was performed as previously described.<sup>36,37</sup> In brief, pseudoviruses were packaged by transient transfection of HEK 293T cells with pNL4-3.Luc.R'E' and pHXB2. The titre of pseudovirus was determined by 2-fold dilution in 1 × 10<sup>5</sup> Ghost cells to final volume of 200 μL. The sample containing the residual inhibitor (50 μL) and pseudovirus (50 μL) was incubated at 37°C for 1 h and then added to Ghost cells (100 μL). The cells were then cultured at 37°C in 5% CO<sub>2</sub> for 48 h, and the relative luminescence units (RLU) were detected with a luciferase kit (Promega, Madison, WI, USA) and luminometer (Ultra 386, Tecan, Durham, NC, USA).

### Assay for sensitivity to proteolytic degradation by proteinase K and pepsin

Assay for neutral proteolytic degradation of N28Fd and ccN28Fd by proteinase K was performed as previously described.<sup>25</sup> Briefly, the proteins (50 μg/mL) were prepared in PBS (pH 7.2) containing 38 microunits/mL proteinase K-agarose. Samples were harvested at different time intervals and centrifuged immediately. The supernatants were stored at -20°C. Assay for acid proteolytic degradation by pepsin (1:10000) was conducted as described before.<sup>24</sup> The proteins (100 μg/mL) were prepared in water adjusted with HCl to pH 1.5. Samples were harvested at different time intervals, neutralized with equal volume of NaOH immediately and incubated at 60°C for 10 min. Samples were kept at -20°C before use. The residual protein concentration and the residual antiviral activity in each sample were detected by ELISA<sup>25</sup> and single-cycle infection as described above.

### Measurement of anti-HIV-1 activity of ccN28Fd

The antiviral activity of the peptides/proteins against infection by HIV-1 IIIB (X4) and enfuvirtide-resistant strains was determined as previously described.<sup>38</sup> Briefly, 1 × 10<sup>4</sup> MT-2 cells were infected with an HIV-1 strain at 100 TCID<sub>50</sub> (50% tissue culture infected dose) in 200 μL culture medium in the absence or presence of an inhibitor at graded concentration overnight. The culture supernatants were then changed with fresh medium. On the fourth day post-infection, 100 μL of culture supernatants was collected from each well, mixed with equal volumes of 5% Triton X-100, and assayed for p24 antigen by ELISA.

The inhibitory activity of the proteins/peptides on infection by HIV-1 Bal strain and HIV-1 HXB2 pseudovirus was determined as described before.<sup>39</sup> Briefly, 1 × 10<sup>4</sup> TZM-bl cells were infected with 100 TCID<sub>50</sub> of viruses with or without the serially diluted inhibitors. On the fourth day post-infection, the culture supernatants were discarded, and the cells were lysed with 50 μL of lysing buffer. Relative luminescence units (RLU) were detected with a luciferase kit (Promega) and luminometer (Ultra 386, Tecan).

The inhibitory activity of the proteins/peptides on infection by primary HIV-1 isolates was determined as previously described.<sup>38</sup> Briefly, the peripheral blood mononuclear cells (PBMC) were isolated from the blood of healthy donors using a standard density gradient (Histopaque-1077, Sigma) centrifugation. After incubation at 37°C for 2 h in 75 cm<sup>2</sup> flasks,

the non-adherent cells were collected and resuspended at  $5 \times 10^5$ /mL in RPMI 1640 medium with 10% fetal bovine serum (FBS), 5  $\mu$ g/mL of PHA and 100 units of interleukin-2/mL, followed by incubation at 37°C for 3 days. The PHA/IL-2-stimulated cells were infected with the primary HIV-1 isolates at a multiplicity of infection (moi) of 0.01 without or with the test inhibitors at graded concentrations. The culture supernatants were harvested 7 days post-infection and assayed for p24 antigen by ELISA.

The half maximal inhibitory concentration ( $IC_{50}$ ) of an inhibitor was calculated using the CalcuSyn software,<sup>40</sup> kindly provided by Dr T. C. Chou at Sloan-Kettering Cancer Center, New York, NY, USA.

### Detection of inhibitory activity on HIV-1 transmission from PBMCs to CEMx174 5.25M7 cells

The inhibitory activity of ccN28Fd on cell-to-cell HIV-1 transmission was determined as previously described.<sup>41</sup> PHA/IL-2-stimulated PBMCs were infected with HIV-1 Bal at moi of 0.01 for 7 days as described above. The infected cells were washed with PBS three times to remove free viral particles and resuspended in culture medium to  $1 \times 10^5$ /mL. Then, 50  $\mu$ L of the cell suspension was incubated with 50  $\mu$ L of ccN28Fd at graded concentration at 37°C for 30 min, followed by adding 100  $\mu$ L of CEMx174 5.25M7 cells ( $2 \times 10^5$ /mL) and co-culturing at 37°C for 3 days. The cells were harvested and lysed for analysis of luciferase activity as described above.

### Combination study

The assays for evaluating HIV-1 IIIB and Bal infection were used to test the synergistic antiviral effect of the ccN28Fd/tenofovir combination as previously described.<sup>42</sup> The anti-HIV-1 activity of ccN28Fd and tenofovir was assessed individually, or in combination, at a fixed molar ratio for the greatest synergism over a range of serial dilutions. The analysis was executed progressively by calculating  $IC_{50}$  (or  $IC_{75}$ ,  $IC_{90}$  and  $IC_{95}$ ) values based on the inhibition curves of single drug or two drugs tested in combination. Then, the combination index was determined by calculating the median effect equation with the CalcuSyn program to assess the synergistic effect of combinations. A combination index of  $< 1$  indicates synergism. Combination index values are interpreted as follows:  $< 0.1$ , very strong synergism; 0.1–0.3, strong synergism; 0.3–0.7, synergism; 0.7–0.85, moderate synergism; and 0.85–0.90, slight synergism. A combination index of 1, or close to 1, indicates additive effects, and a combination index of  $> 1$  indicates antagonism.<sup>43</sup> Dose reduction was obtained by dividing the  $IC_{50}$  value of a peptide tested alone by that of the same agent tested in combination with the other agent.

### Assay for cytotoxicity

The cytotoxicity of ccN28Fd to the target cells (MT-2 cells and TZM-bl cells) used for testing HIV-1 infectivity and human vaginal epithelial cell line (VK2/E6E7) was detected by XTT colorimetric assay as previously described.<sup>44</sup> Briefly, 100  $\mu$ L of ccN28Fd at graded concentrations was added to 100  $\mu$ L cells ( $1 \times 10^5$ /mL) each well. After incubation at 37°C for 4 days, 50  $\mu$ L of XTT solution (1 mg/mL) with 0.02  $\mu$ M phenazine methosulfate (PMS) were added. After 4 h, the absorbance was measured at 450 nm.

### Detection of the effects of hydroxyethylcellulose (HEC) gel, SF and VFS on anti-HIV-1 activities of ccN28Fd

The ccN28Fd gel formulation was prepared by mixing 100  $\mu$ g of ccN28Fd with 0.1 g of the HEC gel (0.1%, w/w). After shaking or stirring at room temperature for 60 min, ccN28Fd was completely dissolved in the 0.1% w/w HEC gel, which was then tested for anti-HIV-1 activity against HIV-1 Bal. The effects of human SF and VFS on anti-HIV-1 activity were detected as previously described.<sup>45,46</sup> SF was obtained by centrifugation of semen at

500 g for 30 min to remove spermatozoa. To avoid the toxic effect of SF and VFS on target cells and viruses, ccN28Fd was first diluted in SF, VFS or PBS at a concentration of 12.5  $\mu$ M. After incubation at 37°C for 60 min, the mixtures were diluted with culture medium 100-fold for testing antiviral activity against HIV-1 Bal and HIV-1 IIIB infection.

## Results

### Design, expression and characterization of ccN28Fd and N28FdE5R

To engineer a recombinant protein with increased stability and anti-HIV-1 activity, we introduced two cysteines into the N terminus of N28Fd (at positions *d* and *e* of the helical wheel of N28, respectively) to form three intermolecular disulphide bonds between the three subunits of a trimer.<sup>47</sup> By so doing, both the N and C termini of the N28-based helical trimer are expected to be stabilized by the intermolecular disulphide bonds and Fd, respectively (Figure 1). For the control protein N28FdE5R, we introduced a mutation, Glu  $\rightarrow$  Arg at position 5 of the Fd fragment in N28Fd, to destabilize the helical trimer by removing an intermolecular salt bridge in Fd.<sup>48</sup> The full sequences and positions of ccN28Fd and N28FdE5R are shown in Figure 1(b).

The plasmids encoding ccN28Fd, N28FdE5R and N28Fd were transformed into *E. coli* strain Rosetta. These proteins were then expressed and purified as described in the Materials and methods section. The newly engineered ccN28Fd was analysed by SDS-PAGE, with N28Fd as a control. The protein samples were treated with 2% SDS at room temperature without boiling. At pH 7.2, both ccN28Fd and N28Fd were trimers; however, at pH 3.0, only ccN28Fd retained trimeric conformation, whereas N28Fd became monomeric. N28FdE5R, as a control, was in monomeric form at pH 7.2 and pH 3.0 (Figure 2). This result suggests that similar to N28Fd, ccN28Fd maintains its trimeric conformation under both neutral and acidic pH, while N28Fd loses its trimeric conformation in an acidic environment.

The recombinant proteins ccN28Fd and N28Fd were further analysed by SVA. The sedimentation coefficient of ccN28Fd and N28Fd was 1.34s and 1.43s, corresponding to 22.6 and 18.3 kDa,

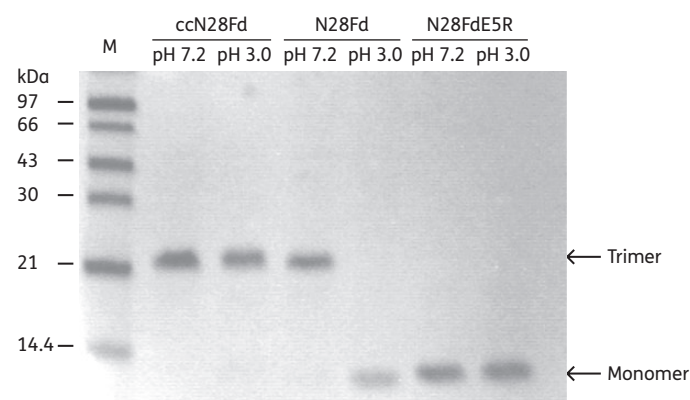


**Figure 2.** SDS-PAGE analysis of ccN28Fd, N28Fd and N28FdE5R. The samples were adjusted to pH 7.2 or pH 3.0 in the presence of 2% SDS and directly loaded on to the gel. Arrows indicate the positions of monomers and trimers. M, protein marker. The experiment was repeated once, and a similar result was obtained.

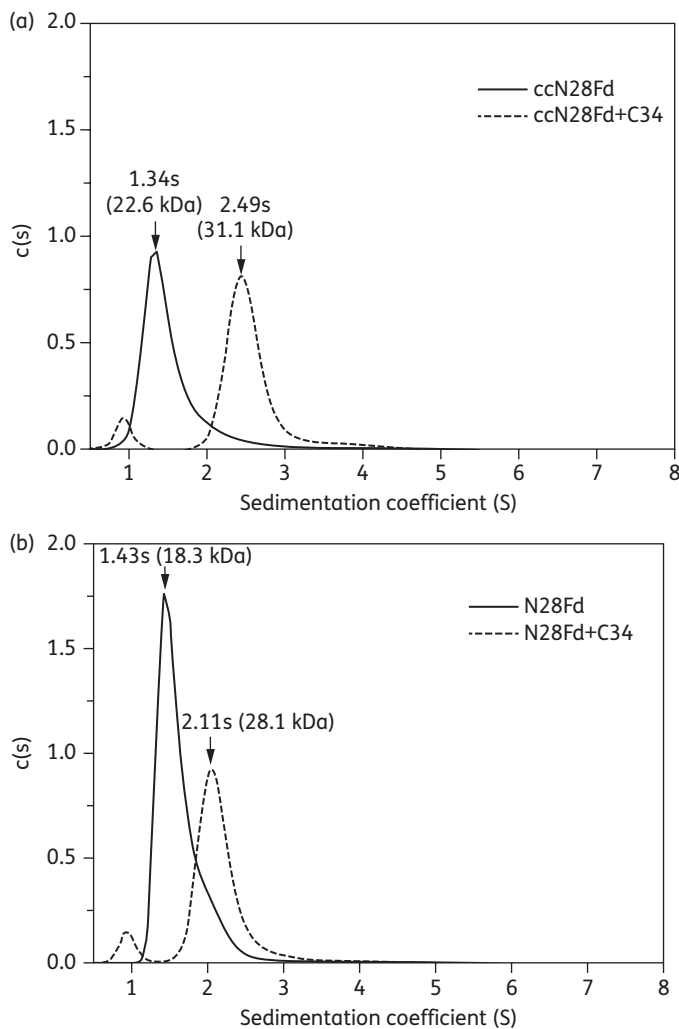


**Figure 3.** Sedimentation velocity analysis of ccN28Fd and the ccN28Fd/C34 mixture (a) and N28Fd and the N28Fd/C34 mixture (b). The recombinant proteins ccN28Fd and N28Fd in 100 mM  $\text{CH}_3\text{COONa}/\text{CH}_3\text{COOH}$  buffer and their complexes with C34 in PBS (pH 7.2) were monitored. The sedimentation coefficient ( $s$ ) and molecular mass (kDa) of each peak are indicated. The experiment was repeated once, and a similar result was obtained.

in agreement with the theoretical molecular mass for a ccN28Fd trimer (20.1 kDa) and N28Fd trimer (19.1 kDa), respectively (Figure 3). The frictional coefficient ( $f/f_0$ ) in SVA reflects shape-distribution of the protein tested. The  $f/f_0$  value, which is calculated from experimental data using the SEDFIT program, allows for estimation of the extent to which the protein shape differs from a compact, unhydrated globular protein of the same mass and density.<sup>49</sup> The  $f/f_0$  value of a globular, hydrated protein is 1.2–1.4, while a moderately elongated protein is 1.6–1.9. The  $f/f_0$  values of ccN28Fd and N28Fd were 1.93 and 1.66, respectively, indicating that the shape of ccN28Fd and N28Fd are moderately elongated.

The CD spectra and thermodynamic stability of these proteins were subsequently analysed. As shown in Figure 4, ccN28Fd and N28Fd exhibited similar secondary structure, i.e. an atypical  $\alpha$ -helix, presumably because of the presence of a  $\beta$ -sheet

domain in Fd.<sup>50</sup> However, ccN28Fd had much higher melting temperature ( $T_m=79^\circ\text{C}$ ) than N28Fd ( $T_m=64^\circ\text{C}$ ), suggesting that ccN28Fd trimer with intermolecular disulphide bonds at its N terminus has much more thermostability than N28Fd.

### Binding of ccN28Fd to the CHR domain of gp41

The ccN28Fd trimer is expected to mimic the pre-hairpin intermediate of HIV-1 gp41 for inhibiting HIV-1 entry into the target cell by binding with the viral gp41 CHR to block the fusogenic six-helix bundle core formation. We thus examined whether ccN28Fd (N28Fd as a control) could interact with C34 by SVA and CD. As analysed by SVA, the sedimentation coefficient of ccN28Fd/C34 complex and N28Fd/C34 complex was 2.49s and 2.11s, corresponding to 31.1 and 28.1 kDa, in agreement with the theoretical molecular mass for a ccN28Fd/C34 six-helix bundle (32.9 kDa) and N28Fd/C34 six-helix bundle (31.9 kDa), respectively (Figure 3). Data from CD analysis indicated that ccN28Fd/C34 complex was more stable ( $T_m=77^\circ\text{C}$ ) than N28Fd/C34 complex ( $T_m=64^\circ\text{C}$ ) (Figure 4). These results suggest that ccN28Fd is able to bind with the gp41 CHR peptide, C34, to form a six-helix bundle core with higher thermostability than that formed by N28Fd and C34.

### Potent antiviral activity of ccN28Fd against a broad spectrum of HIV-1 strains and cell-to-cell transmission of HIV-1

We next tested the anti-HIV-1 activity of ccN28Fd, in comparison with N28Fd and enfuvirtide. As shown in Figure 5(a), ccN28Fd effectively inhibited HIV-1 IIIB (subtype B, X4) infection in MT-2 cells with an  $\text{IC}_{50}$  of 5.1 nM, which is 18.3-fold and 6.4-fold more potent than N28Fd ( $\text{IC}_{50}=93.5$  nM) and enfuvirtide ( $\text{IC}_{50}=32.6$  nM), respectively. The  $\text{IC}_{50}$  value of ccN28Fd for inhibiting infection by HIV-1 Bal (subtype B, R5) infection was 3.7 nM, which is 23-fold and 10.2-fold more potent than N28Fd ( $\text{IC}_{50}=85.1$  nM) and enfuvirtide ( $\text{IC}_{50}=37.6$  nM) (Figure 5b). We further evaluated the antiviral activity of ccN28Fd against a panel of primary HIV-1 isolates of group M, including subtypes A, B, C, D, F, A/E and group O (BCF02). As shown in Table 1, ccN28Fd effectively inhibited these primary isolates with low nanomolar  $\text{IC}_{50}$ , ranging from 3 to 75 nM. We also tested whether ccN28Fd was effective against HIV-1 variants resistant to enfuvirtide, the only FDA-approved HIV-1 entry inhibitor targeting gp41. Five enfuvirtide-resistant strains<sup>51</sup> with mutations in the gp41 NHR region were used in this experiment. HIV-1<sub>NL4-3(36G)V38A</sub> strain with a single mutation was moderately resistant to enfuvirtide ( $\text{IC}_{50}=943$  nM), while those with double mutations, including HIV-1<sub>NL4-3(36G)V38A/N42D</sub>, HIV-1<sub>NL4-3(36G)N42T/N43K</sub> and HIV-1<sub>NL4-3(36G)V38A/N42T</sub> strains, were highly resistant to enfuvirtide ( $\text{IC}_{50}>2000$  nM). Strikingly, ccN28Fd showed high potency against enfuvirtide-resistant strains with  $\text{IC}_{50}$  values in a range of 2–13 nM (Table 2). We then tested whether ccN28Fd inhibited cell-to-cell spread of HIV-1, which permits ongoing replication of drug-resistant HIV-1 strains.<sup>52</sup> As shown in Figure 6, ccN28Fd was highly effective in inhibiting transmission of HIV-1 Bal strain from PBMCs to CEMx174 5.25M7 cells with  $\text{IC}_{50}$  of 30.5 nM. These results suggest that the newly engineered ccN28Fd possesses potent antiviral activity against a broad spectrum of HIV-1 strains of different subtypes (clades A, B, C, D, F and A/E, group O)

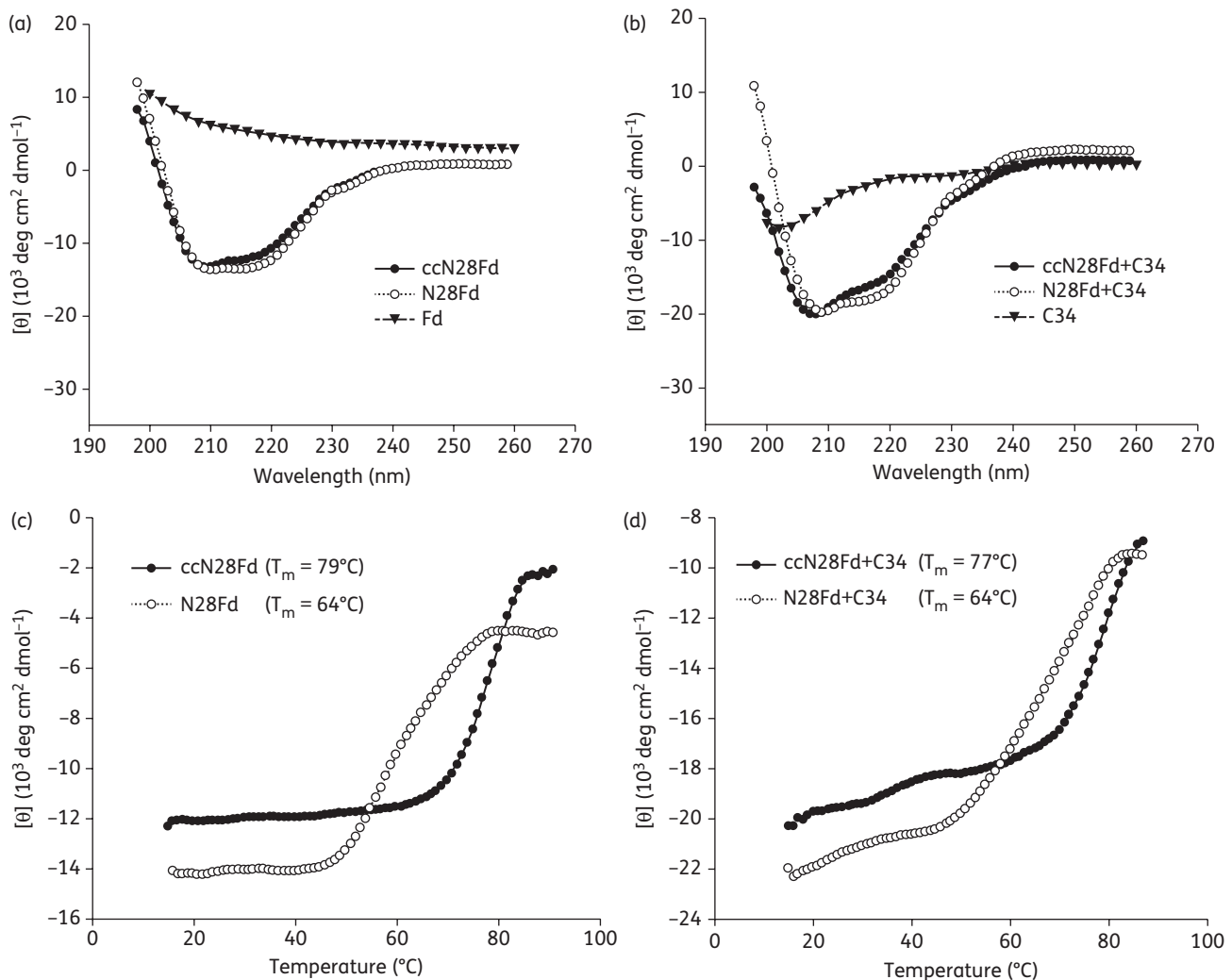


**Figure 4.** CD spectra and thermal denaturation curves of separated NHR proteins, or mixture of NHR proteins and C34, as determined by CD spectroscopy. CD spectroscopy was used to determine the secondary structure of ccN28Fd and N28Fd (a) and the mixture of ccN28Fd and N28Fd with C34, respectively (b). CD spectra of each protein and their complexes with C34 were monitored in PBS, pH 7.2, at ambient temperature. The final concentration of the peptide or protein was  $10 \mu\text{M}$ . The melting temperature ( $T_m$ ) for ccN28Fd or N28Fd (c) and their complexes with C34 (d) are shown in the figure. The experiment was repeated once, and a similar result was obtained.

and phenotypes (X4, X4/R5 and R5) and is also effective in blocking cell-to-cell transmission of HIV-1.

### Combining ccN28Fd with tenofovir resulted in highly potent synergistic anti-HIV-1 activity

The above studies have shown that ccN28Fd could potently inhibit HIV-1 infection by binding to gp41 CHR and blocking HIV-1 entry into host cells. Here we tested the potential cooperative effects of ccN28Fd with tenofovir, an NRTI, as a component in a microbicide in clinical trials. Notably, the combination of ccN28Fd with tenofovir exhibited strong synergism against HIV-1 IIIB (X4) and Bal (R5) strains, with combination index values (combination index at  $\text{IC}_{50}$ ,  $\text{IC}_{75}$ ,  $\text{IC}_{90}$  and  $\text{IC}_{95}$ ) in a range of 0.1 to 0.3 (Table 3). For inhibition of HIV-1 IIIB, dose reductions of corresponding IC (50, 75, 90 and 95) for ccN28Fd and tenofovir in a given

combination were 10.0- to 11.4-fold and 8.6- to 12.8-fold, respectively. For inhibition of HIV-1 Bal, dose reductions were 13- to 16.5-fold and 18.2- to 22.1-fold, respectively. These results suggest that ccN28Fd and tenofovir, which are targeted to the HIV-1 entry and replication stages, respectively, have good potential to be developed as a microbicide combination for preventing sexual transmission of HIV-1.

### High resistance of ccN28Fd to proteolytic degradation by proteinase K and pepsin

Numerous antiviral proteins and peptides have potent anti-HIV-1 activity; however, they rapidly degrade in the vaginal environment with abundant proteolytic enzymes under low pH (3.8–4.4).<sup>27</sup> The engineered protein ccN28Fd, a compact trimeric coiled coil structure stabilized by intermolecular disulphide bonds and Fd, is

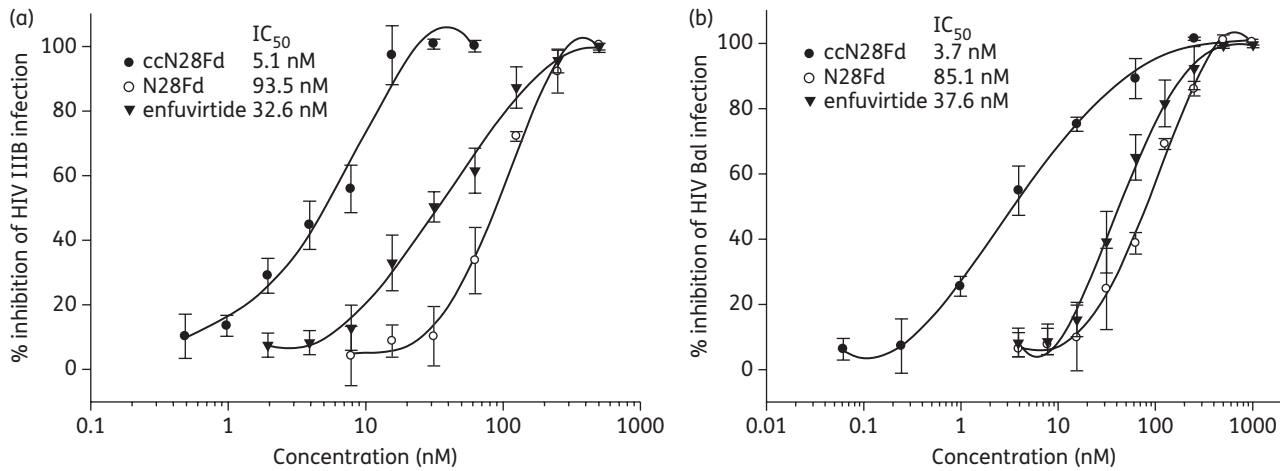


**Figure 5.** Inhibitory activities of ccN28Fd against infection by HIV-1 strains IIIB (a) and Bal (b), in comparison with N28Fd and enfuvirtide. The inhibitory activities of ccN28Fd, N28Fd and enfuvirtide against infection by HIV-1 IIIB (subtype B, X4) in MT-2 cells were determined by ELISA for p24, and their inhibitory activities against infection by HIV-1 Bal (subtype B, R5) in M7 cells were assessed by assay for luciferase activity. The experiment was performed in triplicate. The data are presented as means  $\pm$  SD from a single representative experiment out of two repeats. The IC<sub>50</sub> value of each peptide is shown in the figure.

**Table 1.** Inhibitory effect of ccN28Fd against infection by primary HIV-1 isolates

HIV-1 isolate	Subtype	Tropism	IC <sub>50</sub> (nM)	
			ccN28Fd	enfuvirtide
92UG029	A	X4	3.1 $\pm$ 0.2	1.0 $\pm$ 0.0
94US_33931N	B	R5	24.4 $\pm$ 2.0	7.5 $\pm$ 0.1
93IN101	C	R5	31.0 $\pm$ 3.4	12.4 $\pm$ 0.2
92UG024	D	X4	8.0 $\pm$ 0.2	2.2 $\pm$ 0.0
NP1525	A/E	X4/R5	9.4 $\pm$ 0.1	11.0 $\pm$ 0.0
92TH009	A/E	R5	21.6 $\pm$ 2.5	10.1 $\pm$ 1.9
93/BR/020	F	X4/R5	49.1 $\pm$ 0.4	14.0 $\pm$ 0.1
BCF02	O	R5	75.6 $\pm$ 7.3	30.8 $\pm$ 0.1

The assay was performed in triplicate and repeated at least once. The data are presented as means  $\pm$  SD from one representative experiment. Enfuvirtide was included as a control.

**Table 2.** Inhibitory activity of ccN28Fd against infection by enfuvirtide-resistant HIV-1 strains

HIV-1 strain	IC <sub>50</sub> $\pm$ SD, nM	
	ccN28Fd	enfuvirtide
V38A	4.6 $\pm$ 1.3	943.0 $\pm$ 46.4
V38A/N42D	3.6 $\pm$ 0.3	>2000
N42T/N43K	13.1 $\pm$ 0.3	>2000
V38E/N42S	10.0 $\pm$ 1.8	>2000
V38A/N42T	2.0 $\pm$ 0.0	>2000

The experiment was performed in triplicate and repeated at least once. The data are presented as means  $\pm$  SD from one representative experiment. Enfuvirtide was included as a control.

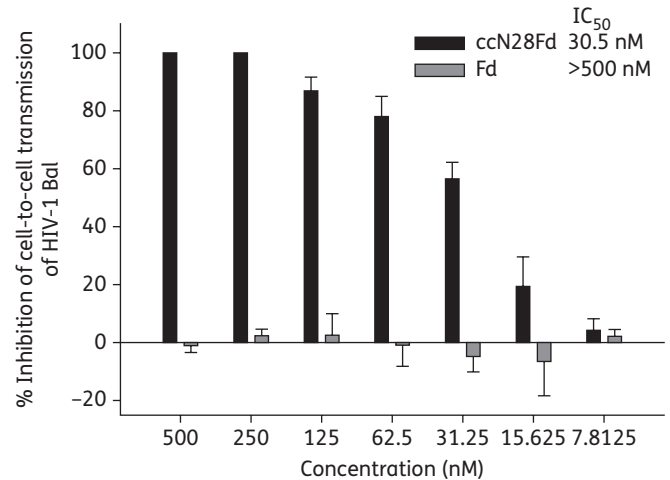


**Figure 6.** ccN28Fd-mediated inhibition of HIV-1 Bal transmission from PBMCs to CEMx174 5.25M7 cells. Inhibition of HIV-1 cell-to-cell transmission was assessed using HIV-1-infected PBMCs that were stimulated with PHA/IL-2 as effective cells and the CD4<sup>+</sup> and CXCR4/CCR5<sup>+</sup> CEMx174 5.25M7 cells as the target cells. HIV-1 infectivity in the target cells was detected 3 days after co-culture of the HIV-1-infected PBMCs and CEMx174 5.25M7 cells using a luciferase assay. Each sample was tested in triplicate, and the experiment was repeated twice. The data are presented as means  $\pm$  SD from a representative experiment. The IC<sub>50</sub> value of each peptide is shown in the figure.

expected to be more resistant to the proteolytic enzymes than N28Fd. We thus compared their sensitivity to proteinase K, a broad-spectrum serine protease, in neutral solution and pepsin in acid solution. As shown in Figure 7, after treatment with 38 microunits/mL proteinase K in PBS (pH 7.2) for 4 h, ccN28Fd retained more than 99% of the original amount and 90% of its anti-HIV-1 activity, while N28Fd was completely degraded and lost its anti-HIV-1 activity. After treatment with 10 nM of pepsin in HCl (pH 1.5)

**Table 3.** Combination index and dose reduction values for inhibition of HIV-1 IIIB and Bal infection by combinations of ccN28Fd and tenofovir

Percentage inhibition	Combination index	ccN28Fd			Tenofovir		
		concentration (nM)			concentration (nM)		
		alone	mixed	dose reduction	alone	mixed	dose reduction
Inhibition of HIV-1 IIIB infection							
50	0.22	5.0	0.5	10.0	2192.7	256.3	8.6
75	0.20	9.7	0.9	10.8	4691.7	472.5	9.9
90	0.18	18.9	1.7	11.1	10038.0	871.1	11.5
95	0.17	29.6	2.6	11.4	16840.0	1320.6	12.8
Inhibition of HIV-1 Bal infection							
50	0.12	3.3	0.2	16.5	1939.0	106.7	18.2
75	0.12	6.5	0.5	13.0	4446.3	227.4	19.6
90	0.12	13.1	1.0	13.0	10196.0	484.5	21.0
95	0.12	21.1	1.6	13.1	17928.0	810.6	22.1

The experiment was performed in triplicate and repeated once. The mean values from one representative experiment are presented. The ratio of the peptide ccN28Fd and tenofovir in combinations is 1:500 (in molecular concentration).

for 4 h, ccN28Fd retained 89% of the original amount and 100% of its anti-HIV-1 activity, while N28Fd retained only 30% of the original amount and completely lost its anti-HIV-1 activity. These results indicate that the newly engineered ccN28Fd is much more resistant to proteolytic degradation by proteinase K and pepsin than the unmodified N28Fd.

### No significant effect of SF, VFS and HEC gel on ccN28Fd-mediated anti-HIV-1 activity

The efficacy of topical microbicides can be affected by human body fluids, such as seminal plasma and vaginal secretions.<sup>53</sup> Therefore, we tested the effect of SF and VFS on the anti-HIV-1 activity of ccN28Fd. As shown in Figure 8, the inhibition activity of ccN28Fd against HIV-1 IIIB and Bal strains was not significantly affected by SF or VFS. The IC<sub>50</sub> values of ccN28Fd for inhibiting HIV-1 IIIB infection in the presence of SF and VFS were 10.33 and 9.51 nM, respectively, while that in PBS control was 11.23 nM. The IC<sub>50</sub> values of ccN28Fd for inhibition of HIV-1 Bal infection in the presence of SF and VFS were 5.39 and 4.79 nM, respectively, while that in PBS control was 4.13 nM. Furthermore, ccN28Fd released from the HEC gel formulation exhibited antiviral potency similar to that in PBS control (Figure S1, available as Supplementary data at JAC Online). These results suggest that ccN28Fd can be formulated in HEC gel as a topical microbicide with potent antiviral activity that is not affected by human seminal and vaginal fluids.

### No significant cytotoxicity of ccN28Fd

An ideal microbicide should have no toxic effect on human cells and tissues, particularly the mucosal tissues in the genital tracts. Using an XTT assay, we tested whether ccN28Fd had any *in vitro* cytotoxicity to the target cells (MT-2 and TZM-bl) used for evaluating anti-HIV-1 activity and the human vaginal epithelial cell lines (VK2/E6E7). As shown in Figure S2 (available as Supplementary data at JAC Online), ccN28Fd did not show significant cytotoxicity to these cells at the concentration as high as 10 µM. This result

suggests that ccN28Fd may not have toxic effect on human immune cells or vaginal/cervical tissues, if it is applied as a topical microbicide.

## Discussion

For developing an HIV-1 fusion/entry inhibitor-based microbicide, we previously designed an NHR-trimer, N28Fd,<sup>25</sup> by fusing the trimerization motif Fd to the C terminus of N28 peptide (Figure 1). As expected, N28Fd exhibits a trimeric conformation and has better anti-HIV-1 activity than N28. However, it is not an ideal anti-HIV microbicide candidate since it is sensitive to low pH and protease treatments, possibly because the N termini of the three N28 peptides in the N28Fd trimer may not be tightly associated. To solve this problem, we engineered a new protein, ccN28Fd, by adding four amino acids, CCGG, to the N terminus of each N28Fd molecule. The two cysteines in one N28Fd molecule are expected to form two disulphide bonds with one of the two cysteines at the N termini of other two N28Fd molecules, respectively, in the ccN28Fd trimer, resulting in the formation of a highly stable NHR-trimer because both ends of the trimer are fixed by disulphide bonds and Fd, respectively (Figure 1).

The designed protein, ccN28Fd, was solubly expressed in prokaryotic *E. coli* with more than 5 mg of protein per litre of culture in laboratory flasks. As expected, ccN28Fd maintained trimeric conformation under both neutral (pH 7.2) and acidic (pH 3.0) conditions, while N28Fd became monomeric at pH 3.0, even though it formed a trimer at pH 7.2 (Figure 2). N28FdE5R, which has an E5R mutation that disrupts the trimerization function of Fd, was in monomeric form at both pH 7.2 and pH 3.0. Sedimentation velocity analysis also confirmed that ccN28Fd was in trimeric form (Figure 3). Although ccN28Fd and N28Fd showed similar atypical α-helix by the presence of β-sheet domain of Fd, the six-helix bundle formed by ccN28Fd and C34 had much higher T<sub>m</sub> value (79°C) than that formed by N28Fd and C34 (64°C), suggesting that the addition of two cysteines to the N terminus of the N28Fd

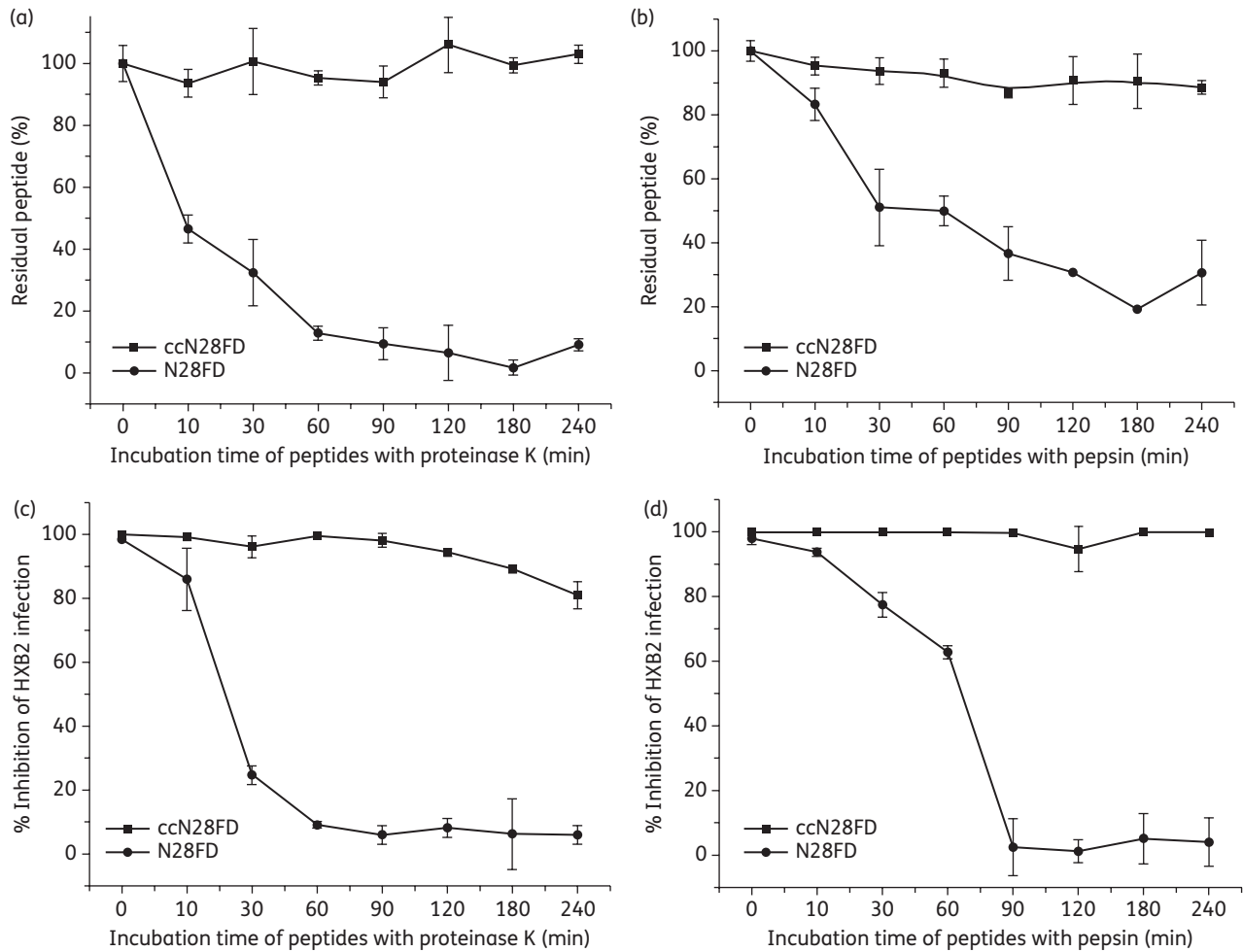


**Figure 7.** Sensitivity of ccN28Fd and N28Fd to proteolytic degradation by proteinase K and pepsin. After digestion by proteinase K at pH 7.2 (a and c) and pepsin at pH 1.5 (b and d), the residual amount of ccN28Fd or N28Fd was detected by a direct ELISA, and the remaining antiviral potency of ccN28Fd or N28Fd was detected by a single-cycle pseudovirus (HXB2) assay. The experiment was performed in triplicate. The data are presented as means  $\pm$  SD from a single representative experiment out of two repeats.

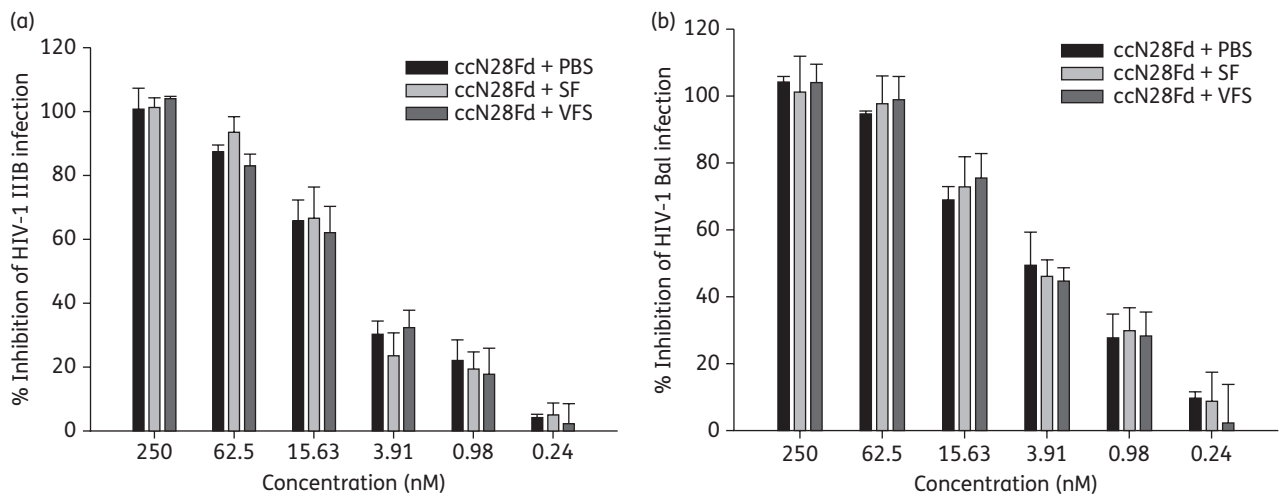


**Figure 8.** Effect of human SF and VFS on the anti-HIV-1 activity of ccN28Fd. The antiviral activities against HIV-1 IIIB (a) and HIV-1 Bal (b) in the presence or absence of SF and VFS were tested using a p24 assay and a luciferase assay, respectively. The experiment was performed in triplicate. The data are presented as means  $\pm$  SD from a single representative experiment out of two repeats.

leads to increased thermostability and the enhanced binding affinity of ccN28Fd to the gp41 CHR region.

Besides strong acidic conditions in the vaginal tract (pH < 4.5), another obstacle for developing vaginally usable protein/peptide-based microbicides is the existence of abundant proteolytic enzymes in the vagina, which may hydrolyse the protein/peptide drugs and shorten their half-lives. Strikingly, ccN28Fd is highly resistant to protease cleavage, compared with N28Fd. After a 4 h treatment with proteinase K, ccN28Fd remained intact with >90% of its anti-HIV-1 activity, while N28Fd was almost completely degraded with the loss of most of its antiviral activity (Figure 7). Similarly, ccN28Fd was highly resistant to treatment by pepsin in HCl (pH 1.5) for 4 h, whereas N28Fd retained only 30% of the original amount and fully lost its anti-HIV-1 activity. These results indicate that ccN28Fd may have much longer half-life than N28Fd when it is vaginally applied as a topical microbicide.

Interestingly, stabilization of the NHR-trimeric coiled coil also resulted in significantly increased anti-HIV-1 potency of ccN28Fd. The inhibitory activity of ccN28Fd against infection by HIV-1 IIIB (X4 virus) and Bal (R5 virus) was 18.3- and 23-fold higher than that of N28Fd, respectively, and 6.4- and 10.2-fold higher than that of enfuvirtide (Figure 5). One possible mechanism of the increased antiviral activity is that the three monomers of ccN28Fd associate with each other more tightly than those in N28Fd, which causes the decreased hydrodynamic radius and makes it much easier for the trimer of ccN28Fd to access to the CHR of HIV-1 gp41 than the trimer of N28Fd.

We also found that ccN28Fd was highly effective (IC<sub>50</sub> = 30.5 nM) in blocking the transmission of HIV-1 Bal from PBMCs to CEMx174 5.25M7 cells (Figure 6). Unlike ionic polymer-based microbicide candidates that are much less effective against R5 viruses, these results suggest that ccN28Fd has similar efficacy against both R5 and X4 viruses. Moreover, ccN28Fd could inhibit infection by a broad spectrum of primary HIV-1 isolates with distinct genotypes (subtypes A, B, C, D, A/E, F and O) and phenotypes (X4, X4/R5 and R5) in a range of 3–75 nM (Table 1). It is also effective in inhibiting infection by enfuvirtide-resistant strains (Table 2). Thus, for the development of anti-HIV microbicides, these results indicate that ccN28Fd has more potential than either N28Fd or enfuvirtide since it is highly effective against a broad spectrum of HIV-1 strains, including those resistant to the currently used anti-HIV drugs, such as enfuvirtide.

One important lesson that we have learned from others' experience in developing surfactant-based microbicides is that toxicity of the surfactants to vaginal mucosal tissue is responsible for the failure of the trials on these microbicides.<sup>54</sup> Therefore, in this study, we tested potential cytotoxicity of ccN28F to the human vaginal epithelial cell lines (VK2/E6E7) and the target cells (MT-2 and TZM-bl) that we used for testing antiviral activity. As shown in Figure S2, ccN28Fd exhibited no significant *in vitro* cytotoxicity to these cells at a concentration as high as 10 μM, suggesting that it may also have no toxic effect on the vaginal/cervical tissues when it is used vaginally as a topical microbicide.

Vaginal microbicides are commonly administered by formulating an aqueous mucoadhesive gel.<sup>55–57</sup> The antiviral potency of an ideal microbicide should not be significantly decreased when it is released from the gel or in the presence of human vaginal secretion or semen. Our study showed that solution from ccN28Fd gel formulation remained at a high level of antiviral potency against HIV-1 infection and that the presence of vaginal fluid simulants and seminal fluid had no significant effect on the antiviral potency of ccN28Fd

(Figure S1, available as Supplementary data at JAC Online), suggesting that ccN28F is suitable for further development as an effective and safe anti-HIV microbicide.

Because of long-term application of ART in HIV/AIDS patients, the emergence of multidrug-resistant HIV-1 variants has posed a challenge for the design of highly effective microbicides. Consequently, the combination of microbicides consisting of anti-HIV agents with different mechanisms of action is expected to have synergistic anti-HIV-1 activity against a broad spectrum of HIV-1 strains, including those resistant to the currently used anti-HIV drugs.<sup>17</sup> Veazey et al.<sup>21</sup> reported that the CCR5 receptor antagonist CMPD167 could fully protect macaques from infection by SHIV (162P4), but only in combination with BMS-378806, an HIV attachment targeting gp120, and C52-L, an HIV fusion inhibitory peptide targeting gp41. In the present study, we demonstrated that the combination of ccN28Fd with tenofovir, an NRTI, resulted in strong synergism against HIV-1 IIIB (X4 virus) and Bal (R5 virus) with combination index values in the range of 0.1–0.3 (Table 3) and dose reductions ranging from 10- to 22-fold. These results suggest that ccN28Fd, as a stable HIV entry inhibitor targeting viral gp41, can be combined with an NRTI or NNRTI to develop a highly effective and safe microbicide combination for preventing sexual transmission of HIV.

## Acknowledgements

We are grateful to Dr Linqi Zhang at Tsinghua University for providing the Ghost cell line and plasmids of pseudovirus. We also thank Dr Lifeng Cai at the Beijing Institute of Pharmacology and Toxicology for his assistance in CD measurements.

## Funding

This work was supported by grants from the National Natural Science Foundation of China (81173098 to S. J., 81271823 to Y. H. C. and 81102476 to L. L.); National Fund for Talent Training in Basic Science (1030622) to Y. H. C., and the 'Chen Guang' Project of SMEC and SEDF (11CG03) to L. L.

## Transparency declarations

None to declare.

## Supplementary data

Figures S1 and S2 are available as Supplementary data at JAC Online (<http://jac.oxfordjournals.org/>).

## References

- UNAIDS. AIDS Epidemic Update. [http://data.unaids.org/pub/report/2009/jc1700\\_epi\\_update\\_2009\\_en.pdf](http://data.unaids.org/pub/report/2009/jc1700_epi_update_2009_en.pdf) (3 May, 2013, date last accessed).
- UNAIDS. Redefining AIDS in Asia. [http://data.unaids.org/pub/Report/2008/20080326\\_report\\_commission\\_aids\\_en.pdf](http://data.unaids.org/pub/Report/2008/20080326_report_commission_aids_en.pdf) (3 May, 2013, date last accessed).
- Roehr B. Microbicide offers no protection against HIV infection. *Br Med J* 2009; **339**: b5538.
- McGowan I. Microbicides for HIV prevention: reality or hope? *Curr Opin Infect Dis* 2010; **23**: 26–31.

- 5 Bollen LJM, Blanchard K, Kilmarx PH *et al.* No increase in cervicovaginal proinflammatory cytokines after Carraguard use in a placebo-controlled randomized clinical trial. *J Acquir Immune Defic Syndr* 2008; **47**: 253–7.
- 6 Perotti ME, Pirovano A, Phillips DM. Carrageenan formulation prevents macrophage trafficking from vagina: implications for microbicide development. *Biol Repro* 2003; **69**: 933–9.
- 7 Van Damme L, Govinden R, Mirembe FM *et al.* Lack of effectiveness of cellulose sulfate gel for the prevention of vaginal HIV transmission. *N Engl J Med* 2008; **359**: 463–72. Erratum in: *N Engl J Med* 2008; **359**: 877.
- 8 Check E. Scientists rethink approach to HIV gels. *Nature* 2007; **446**: 12.
- 9 Keller MJ, Herold BC. Understanding basic mechanisms and optimizing assays to evaluate the efficacy of vaginal microbicides. *Sex Transm Dis* 2009; **36**: S92–S5.
- 10 Zhu TF, Mo HM, Wang N *et al.* Genotypic and phenotypic characterization of HIV-1 in patients with primary infection. *Science* 1993; **261**: 1179–81.
- 11 Royce RA, Sena A, Cates W *et al.* Current concepts: sexual transmission of HIV. *N Engl J Med* 1997; **336**: 1072–8.
- 12 De Clercq E. Acyclic nucleoside phosphonates: past, present and future. Bridging chemistry to HIV, HBV, HCV, HPV, adeno-, herpes-, and poxvirus infections: the phosphonate bridge. *Biochem Pharmacol* 2007; **73**: 911–22.
- 13 Rohan LC, Moncla BJ, Ayudhya R *et al.* In vitro and ex vivo testing of tenofovir shows it is effective as an HIV-1 microbicide. *PLoS One* 2010; **5**: e9310.
- 14 Das K, Clark AD, Lewi PJ *et al.* Roles of conformational and positional adaptability in structure-based design of TMC125-R165335 (etravirine) and related non-nucleoside reverse transcriptase inhibitors that are highly potent and effective against wild-type and drug-resistant HIV-1 variants. *J Med Chem* 2004; **47**: 2550–60.
- 15 Woolfson AD, Malcolm RK, Morrow RJ *et al.* Intravaginal ring delivery of the reverse transcriptase inhibitor TMC 120 as an HIV microbicide. *Int J Pharm* 2006; **325**: 82–9.
- 16 Abdool Karim Q, Abdool Karim SS, Frohlich JA *et al.* Effectiveness and safety of tenofovir gel, an antiretroviral microbicide, for the prevention of HIV infection in women. *Science* 2010; **329**: 1168–74.
- 17 Garg AB, Nuttall J, Romano J. The future of HIV microbicides: challenges and opportunities. *Antivir Chem Chemother* 2009; **19**: 143–50.
- 18 Wild CT, Shugars DC, Greenwell TK *et al.* Peptides corresponding to a predicative alpha-helical domain of human-immunodeficiency virus type-1 gp41 are potent inhibitors of virus-infection. *Proc Natl Acad Sci USA* 1994; **91**: 9770–4.
- 19 Lalezari JP, Henry K, O'Hearn M *et al.* Enfuvirtide, an HIV-1 fusion inhibitor, for drug-resistant HIV infection in North and South America. *N Engl J Med* 2003; **348**: 2175–85.
- 20 Lazzarin A, Clotet B, Cooper D *et al.* Efficacy of enfuvirtide in patients infected with drug-resistant HIV-1 in Europe and Australia. *N Engl J Med* 2003; **348**: 2186–95.
- 21 Veazey RS, Klasse PJ, Schader SM *et al.* Protection of macaques from vaginal SHIV challenge by vaginally delivered inhibitors of virus-cell fusion. *Nature* 2005; **438**: 99–102.
- 22 Li L, Ben Y, Yuan S *et al.* Efficacy, stability, and biosafety of sifuvirtide gel as a microbicide candidate against HIV-1. *PLoS One* 2012; **7**: e37381.
- 23 Harman S, Herrera C, Armanasco N *et al.* Preclinical evaluation of the HIV-1 fusion inhibitor L'644 as a potential candidate microbicide. *Antimicrob Agents Chemother* 2012; **56**: 2347–56.
- 24 Bird GH, Madani N, Perry AF *et al.* Hydrocarbon double-stapling remedies the proteolytic instability of a lengthy peptide therapeutic. *Proc Natl Acad Sci USA* 2010; **107**: 14093–8.
- 25 Chen X, Lu L, Qi Z *et al.* Novel recombinant engineered gp41 N-terminal heptad repeat trimers and their potential as anti-HIV-1 therapeutics or microbicides. *J Biol Chem* 2010; **285**: 25506–15.
- 26 Kilby JM, Lalezari JP, Eron JJ *et al.* The safety, plasma pharmacokinetics, and antiviral activity of subcutaneous enfuvirtide (T-20), a peptide inhibitor of gp41-mediated virus fusion, in HIV-infected adults. *AIDS Res Hum Retrovir* 2002; **18**: 685–93.
- 27 Rohan LC, Sassi AB. Vaginal drug delivery systems for HIV prevention. *AAPS J* 2009; **11**: 78–87.
- 28 Hunter CA, Lu XJ. Construction of double-helical DNA structures based on dinucleotide building blocks. *J Biomol Struct Dyn* 1997; **14**: 747–56.
- 29 Eckert DM, Kim PS. Mechanisms of viral membrane fusion and its inhibition. *Annu Rev Biochem* 2001; **70**: 777–810.
- 30 Eckert DM, Malashkevich VN, Hong LH *et al.* Inhibiting HIV-1 entry: discovery of D-peptide inhibitors that target the gp41 coiled-coil pocket. *Cell* 1999; **99**: 103–15.
- 31 Bewley CA, Louis JM, Ghirlando R *et al.* Design of a novel peptide inhibitor of HIV fusion that disrupts the internal trimeric coiled-coil of gp41. *J Biol Chem* 2002; **277**: 14238–45.
- 32 Liu SW, Lu H, Niu J *et al.* Different from the HIV fusion inhibitor C34, the anti-HIV drug fuzeon (T-20) inhibits HIV-1 entry by targeting multiple sites in gp41 and gp120. *J Biol Chem* 2005; **280**: 11259–73.
- 33 Owen DH, Katz DF. A vaginal fluid simulant. *Contraception* 1999; **59**: 91–5.
- 34 Lu L, Tong P, Yu XW *et al.* HIV-1 variants with a single-point mutation in the gp41 pocket region exhibiting different susceptibility to HIV fusion inhibitors with pocket- or membrane-binding domain. *Biochim Biophys Acta-Biomembr* 2012; **1818**: 2950–7.
- 35 Shu W, Liu J, Ji H *et al.* Helical interactions in the HIV-1 gp41 core reveal structural basis for the inhibitory activity of gp41 peptides. *Biochemistry* 2000; **39**: 1634–42.
- 36 Geuenich S, Goffinet C, Venzke S *et al.* Aqueous extracts from peppermint, sage and lemon balm leaves display potent anti-HIV-1 activity by increasing the virion density. *Retrovirology* 2008; **5**: 27.
- 37 Wang J, Tong P, Lu L *et al.* HIV-1 gp41 Core with exposed membrane-proximal external region inducing broad HIV-1 neutralizing antibodies. *PLoS One* 2011; **6**: e18233.
- 38 Wild J, Kamath-Loeb A, Ziegelhoffer E *et al.* Partial loss of function mutations in DnaK, the Escherichia coli homologue of the 70-kDa heat shock proteins, affect highly conserved amino acids implicated in ATP binding and hydrolysis. *Proc Natl Acad Sci USA* 1992; **89**: 7139–43.
- 39 Li L, He L, Tan S *et al.* 3-Hydroxyphthalic anhydride-modified chicken ovalbumin exhibits potent and broad anti-HIV-1 activity: a potential microbicide for preventing sexual transmission of HIV-1. *Antimicrob Agents Chemother* 2010; **54**: 1700–11.
- 40 Chatterjee S, Jiang W, Emerson SD *et al.* The backbone structure of the major cold-shock protein CS7.4 of Escherichia coli in solution includes extensive  $\beta$ -sheet structure. *J Biochem* 1993; **114**: 663–9.
- 41 Li L, Qiao P, Yang J *et al.* Maleic anhydride-modified chicken ovalbumin as an effective and inexpensive anti-HIV microbicide candidate for prevention of HIV sexual transmission. *Retrovirology* 2010; **7**: 37.
- 42 Pan CG, Cai LF, Lu H *et al.* Combinations of the first and next generations of human immunodeficiency virus (HIV) fusion inhibitors exhibit a highly potent synergistic effect against enfuvirtide-sensitive and -resistant HIV type 1 strains. *J Virol* 2009; **83**: 7862–72.
- 43 Chou TC. Theoretical basis, experimental design, and computerized simulation of synergism and antagonism in drug-combination studies. *Pharmacol Rev* 2006; **58**: 621–81. Erratum in: *Pharmacol Rev* 2007; **59**: 124.

- 44** Zhu Y, Lu L, Xu L et al. Identification of a gp41 core-binding molecule with homologous sequence of human TNNT3K-like protein as a novel human immunodeficiency virus type 1 entry inhibitor. *J Virol* 2010; **84**: 9359–68.
- 45** Fernandez-Romero JA, Thorn M, Turville SG et al. Carrageenan/MIV-150 (PC-815), a combination microbicide. *Sex Transm Dis* 2007; **34**: 9–14.
- 46** Fletcher PS, Harman SJ, Boothe AR et al. Preclinical evaluation of lime juice as a topical microbicide candidate. *Retrovirology* 2008; **5**: 3.
- 47** Louis JM, Bewley CA, Clore GM. Design and properties of N-CCG-gp41, a chimeric gp41 molecule with nanomolar HIV fusion inhibitory activity. *J Biol Chem* 2001; **276**: 29485–9.
- 48** Habazettl J, Reiner A, Kiefhaber T. NMR Structure of a monomeric intermediate on the evolutionarily optimized assembly pathway of a small trimerization domain. *J Mol Biol* 2009; **389**: 103–14.
- 49** Lej-Garolla B, Mauk AG. Self-association and chaperone activity of Hsp27 are thermally activated. *J Biol Chem* 2006; **281**: 8169–74.
- 50** Papanikolopoulou K, Forge V, Goeltz P et al. Formation of highly stable chimeric trimers by fusion of an adenovirus fiber shaft fragment with the foldon domain of bacteriophage T4 fibrin. *J Biol Chem* 2004; **279**: 8991–8.
- 51** Rimsky LT, Shugars DC, Matthews TJ. Determinants of human immunodeficiency virus type 1 resistance to gp41-derived inhibitory peptide. *J Virol* 1998; **72**: 986–93.
- 52** Sigal A, Kim JT, Balazs AB et al. Cell-to-cell spread of HIV permits ongoing replication despite antiretroviral therapy. *Nature* 2011; **477**: 95–8.
- 53** Neurath AR, Strick N, Li YY. Role of seminal plasma in the anti-HIV-activity of candidate microbicides. *BMC Infect Dis* 2006; **6**: 150.
- 54** Hillier SL, Moench T, Shattock R et al. In vitro and in vivo: the story of Nonoxonyl 9. *J Acquir Immune Defic Syndr* 2005; **39**: 1–8.
- 55** Nel AM, Coplan P, van de Wijgert JH et al. Safety, tolerability, and systemic absorption of dapivirine vaginal microbicide gel in healthy, HIV-negative women. *AIDS* 2009; **23**: 1531–8.
- 56** Veazey RS, Ketas TJ, Dufour J et al. Protection of rhesus macaques from vaginal infection by vaginally delivered maraviroc, an inhibitor of HIV-1 entry via the CCR5 co-receptor. *J Infect Dis* 2010; **202**: 739–44.
- 57** Tsibris AM, Pal U, Schure AL et al. SHIV-162P3 infection of rhesus macaques given maraviroc gel vaginally does not involve resistant viruses. *PLoS One* 2011; **6**: e28047.